

Electronic Supplementary Information (ESI)

Rationally-designed self-shaped ceramics through heterogeneous green body compositions

Zizhen Ding^{a,c}, Hala Zreiqat^{b,c}, Mohammad Mirkhalaf^{a,c}*

^a School of Mechanical, Medical and Process Engineering, Queensland University of Technology,
2 George St Brisbane, QLD 4000 Australia.

^b Biomaterials and Tissue Engineering Research Unit, School of Biomedical Engineering, The
University of Sydney, NSW 2006, Australia.

^c Australian Research Council Training Centre for Innovative Bioengineering, Sydney, NSW 2006,
Australia.

*Corresponding author: mohammad.mirkhalaf@qut.edu.au

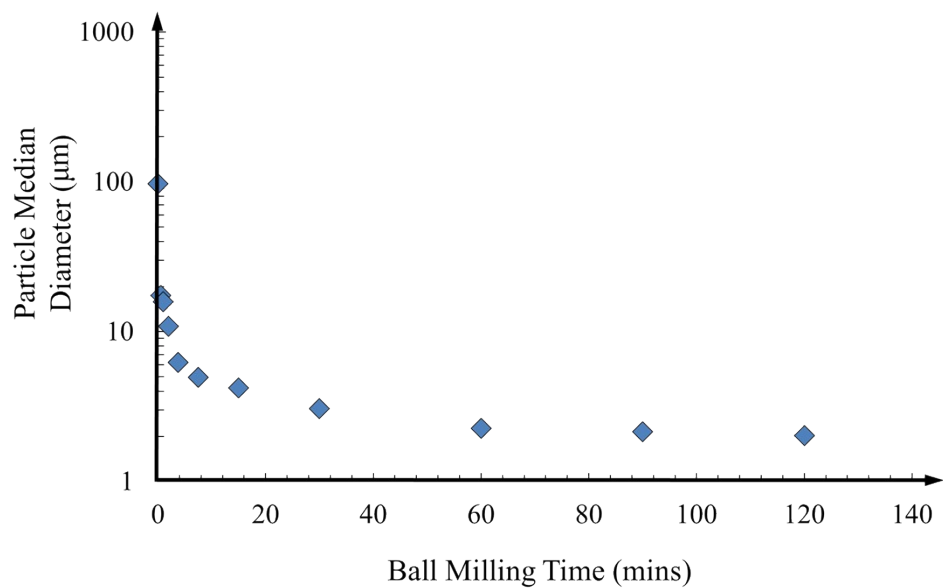


Fig. S1. The alumina particle median diameter profile measured in μm with different ball milling process times (mins).

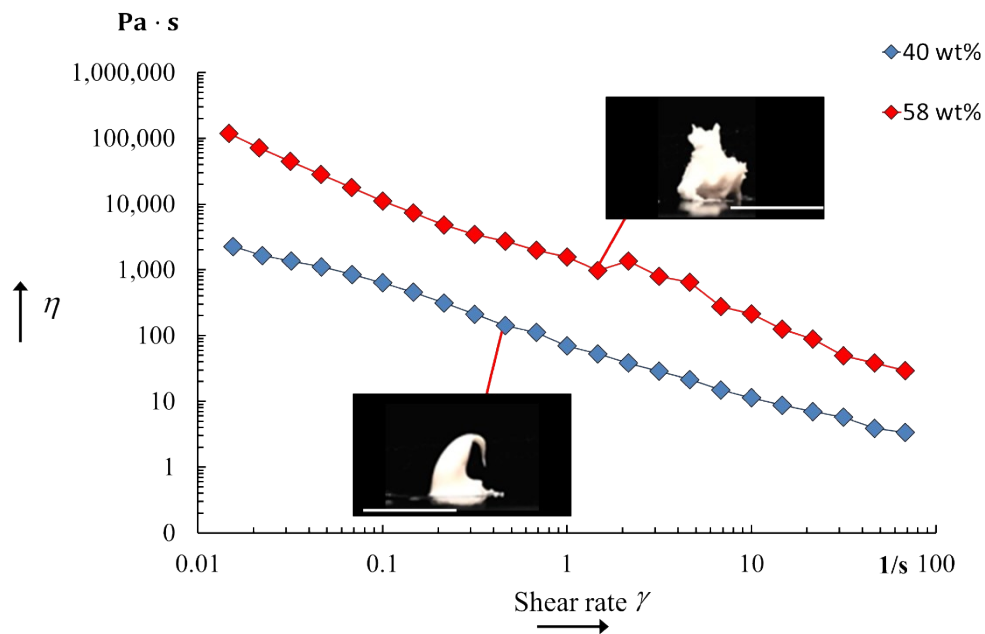


Fig. S2. The rheology behavior of resin with 40 wt% ceramic particle concentration and resin with 58 wt% ceramic particle concentrations. Scale bars indicate 12 mm.

The bending model:

The condition for the equilibrium of a section of the bilayer after sintering is:

$$M_1 + M_2 = \frac{Pt^1}{2} \quad \text{S1}$$

Where M_1 and M_2 are the internal moments, and P is the internal force in the layers. Note that P must be the same in both layers to satisfy the equilibrium. t^1 is the total thickness of the bilayer after sintering. The notations are also shown in **Fig. S3**.

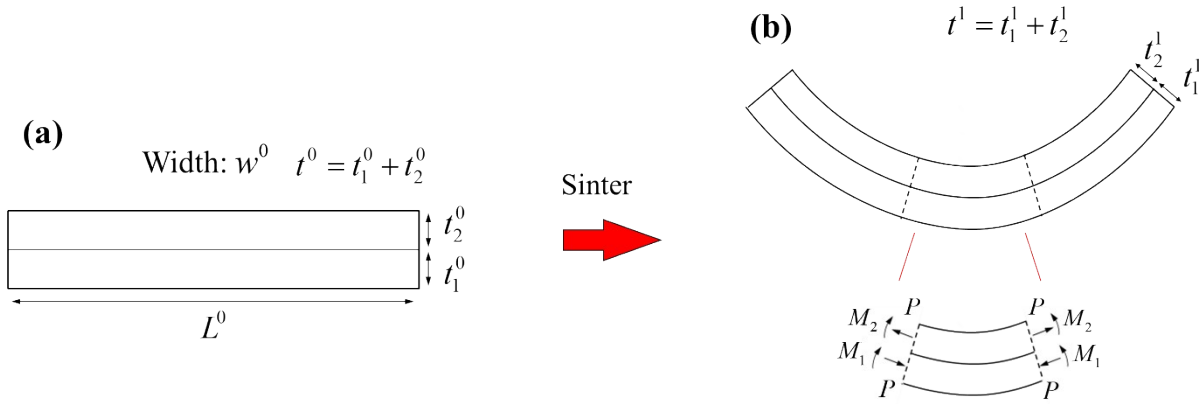


Fig. S3. The bilayer beam. (a) before and (b) after sintering and the notations for the dimensions, forces, and moments.

In the Timoshenko model for bilayers¹, one of the assumptions is that the thickness of the layers does not change significantly. In our systems, however, the shrinkage ratio of the layers was quite large and reached values as high as $\sim 50\%$. Therefore, the initial thickness could not be used in the derivation of the radius of curvature ρ . Since there is no force acting perpendicular to the curvilinear direction of the curved beam in this system, the thickness of the layers after shape changes is:

$$\begin{cases} t_1^1 = t_1^0 (1 + \beta_1) \\ t_2^1 = t_2^0 (1 + \beta_2) \end{cases} \quad \text{S2}$$

Where β_1 and β_2 are shrinkage ratio of the individual layers, t_1^0 and t_2^0 are the thickness of the layers before sintering, t_1^1 and t_2^1 are the thickness of the layers after sintering. SEM images of the bending samples (see **Fig. S15**) confirmed that Equation S2 provides a good prediction of the thickness of bilayers after sintering. Our following equation is related to the deformation of the bilayer: from linear elasticity, the radius of curvature is related to the moments through:

$$\frac{1}{\rho} = \frac{M_1}{E_1 I_1} = \frac{M_2}{E_2 I_2} \quad \text{S3}$$

Where I_1 and I_2 are the second moment of inertia of the cross-sections after sintering:

$$\begin{cases} I_1 = \frac{w^0 (t_1^1)^3}{12} \\ I_2 = \frac{w^0 (t_2^1)^3}{12} \end{cases} \quad \text{S4}$$

Also, the length of the line at the connection between the two beams (centerline) must be the same in both beams and therefore:

$$\beta_1 - \frac{P}{E_1 t_1^1 w^0} - \frac{t_1^1}{2\rho} = \beta_2 + \frac{P}{E_2 t_2^1 w^0} + \frac{t_2^1}{2\rho} \quad \text{S5}$$

The three terms of Equation S5 respectively represent the length change due to sintering, internal load, and bending. By combining Equations S1 and S3, we have:

$$P \frac{t^1}{2} = \frac{E_1 I_1}{\rho} + \frac{E_2 I_2}{\rho} \quad \text{S6}$$

By combining Equations S4, S5, and S6, the radius of curvature can be expressed as:

$$\frac{\rho}{t^1} = \frac{\left(\frac{E_1}{E_2} \left(\frac{t_1^1}{t_2^1} \right)^3 + \left(\frac{t_1^1}{t_2^1} \right)^2 + \frac{E_2}{E_1} \frac{t_2^1}{t_1^1} + 1 \right) + 3 \left(1 + \frac{t_1^1}{t_2^1} \right)^2}{6(\beta_1 - \beta_2) \left(1 + \frac{t_1^1}{t_2^1} \right)^2} \quad \text{S7}$$

Also, from Equation S2, we have:

$$\begin{cases} \frac{t_1^1}{t_2^1} = \frac{(1 + \beta_1) t_1^0}{(1 + \beta_2) t_2^0} \\ \frac{t^1}{t^0} = 1 + \frac{1}{1 + t_2^0/t_1^0} \beta_1 + \frac{1}{1 + t_1^0/t_2^0} \beta_2 \end{cases} \quad \text{S8}$$

By setting $\alpha = \frac{(1 + \beta_1)}{(1 + \beta_2)}$, $m = \frac{t_1^0}{t_2^0}$, and $n = \frac{E_1}{E_2}$, Equation S7 can be written as:

$$\frac{\rho}{t^0} = \left(1 + \frac{m}{1 + m} \beta_1 + \frac{1}{1 + m} \beta_2 \right) \frac{(\alpha^3 n m^3 + \alpha^2 m^2 + 1/\alpha n m + 1) + 3(1 + \alpha m)^2}{6(\beta_1 - \beta_2)(1 + \alpha m)^2} \quad \text{S9}$$

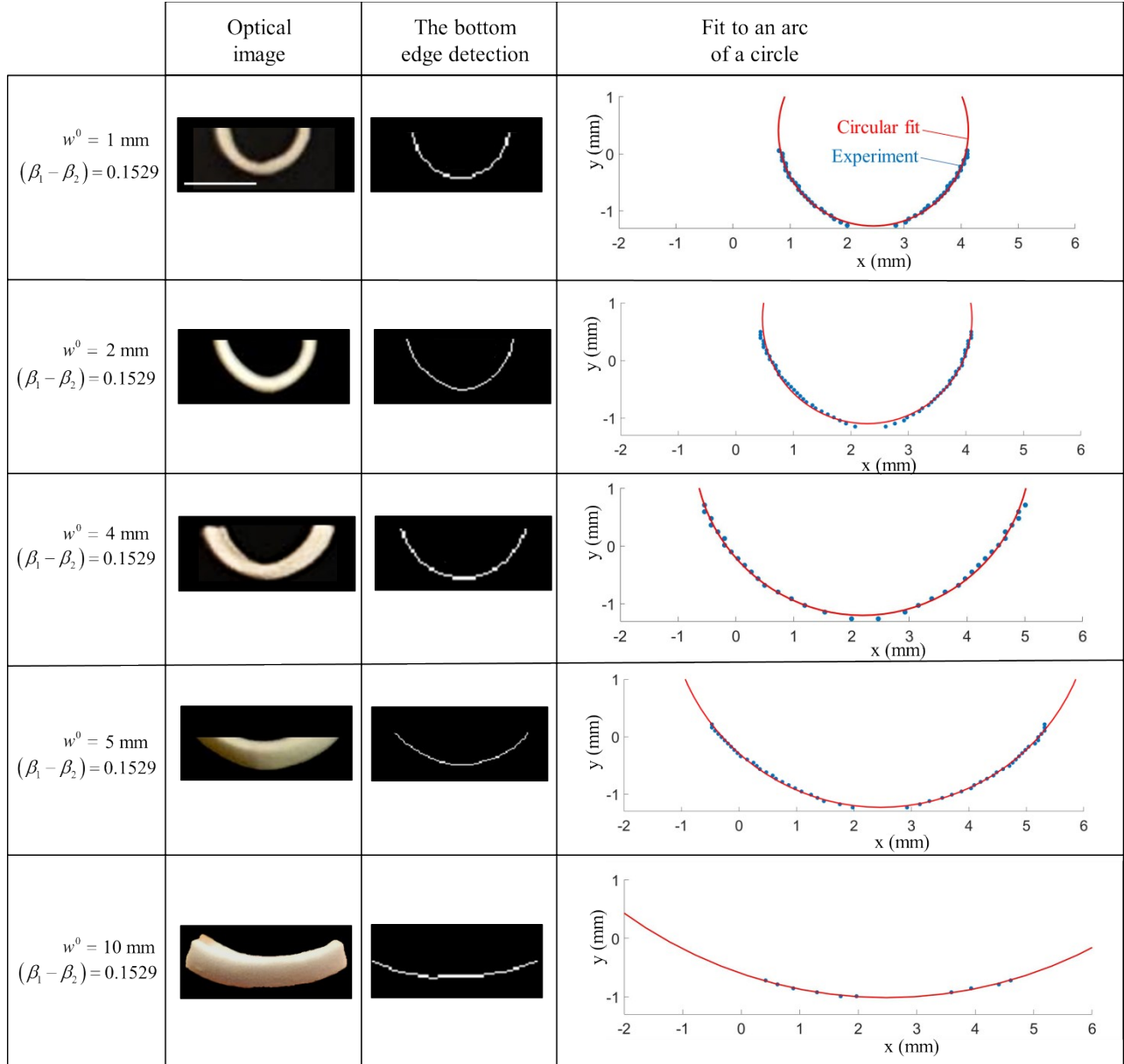


Fig. S4. The optical images, bottom edge detection image, and MATLAB generated arc fitting image of the bending samples with thickness $t^0 = 0.6 \text{ mm}$, length $L^0 = 10 \text{ mm}$, and $(\beta_1 - \beta_2) = 0.1529$ between layers but with widths $w^0 = 1, 2, 4, 5, 10 \text{ mm}$. Scale bar indicates 2 mm.

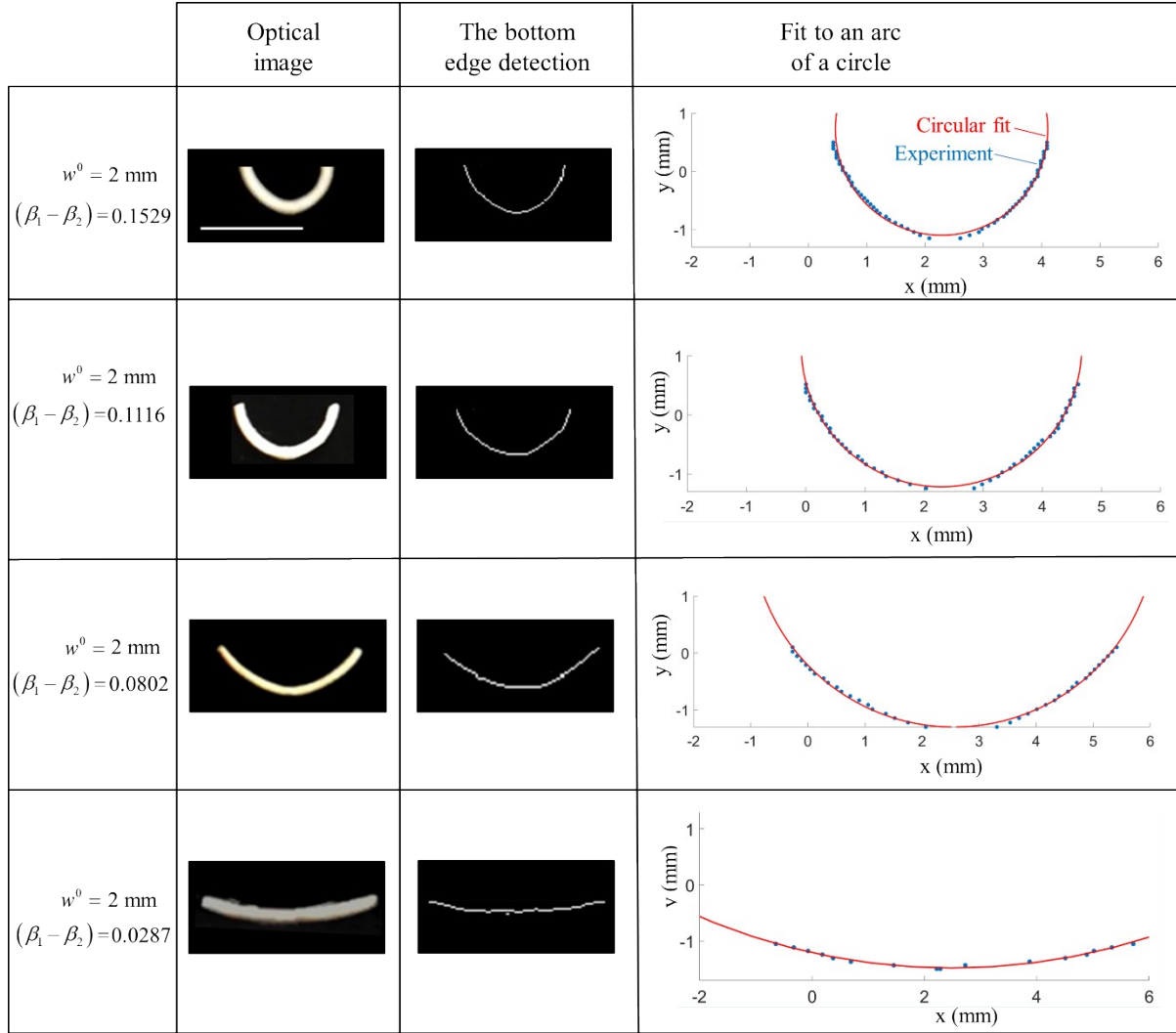


Fig. S5. The optical image, bottom edge detection image, and the MATLAB generated arc fitting image of the bending samples with $w^0 = 2 \text{ mm}$, $t^0 = 0.6 \text{ mm}$, and $L^0 = 10 \text{ mm}$ but with $(\beta_1 - \beta_2) = 0.1529, 0.1116, 0.0802$, and 0.0287 between layers. Scale bars indicate 4 mm .

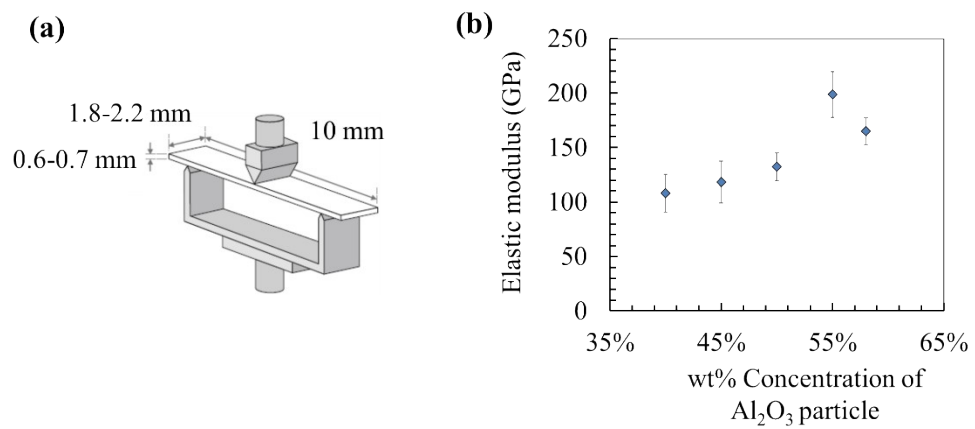


Fig. S6. (a) the test set up for the sintered beams; (b) the elastic modulus of the beams.

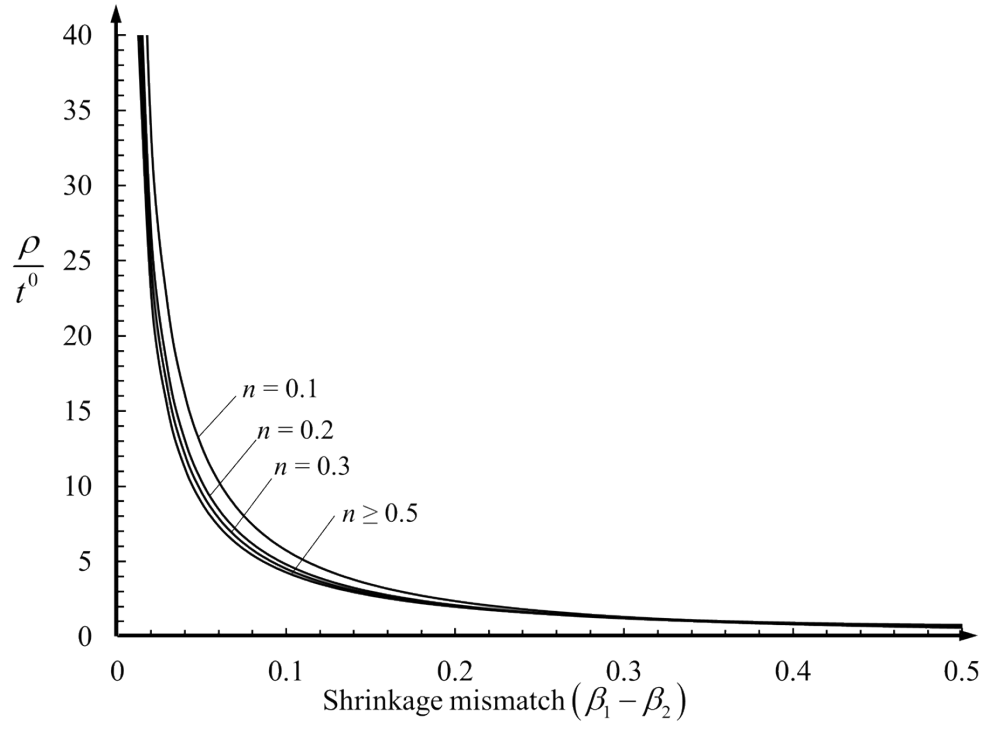


Fig. S7. The model prediction for different n values as a function of shrinkage mismatch $(\beta_1 - \beta_2)$ between the layers.

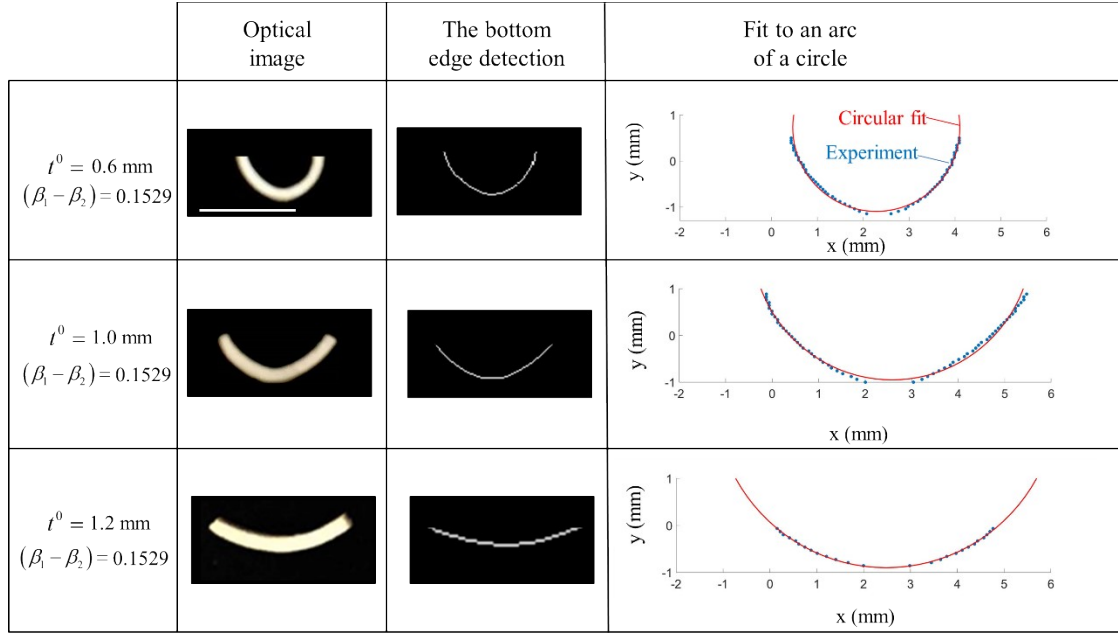


Fig. S8. The optical image, bottom edge detection image, and the MATLAB generated arc fitting image of the bending samples with $w^0 = 2 \text{ mm}$, $L^0 = 10 \text{ mm}$, and $(\beta_1 - \beta_2) = 0.1529$ between layers but with $t^0 = 0.6, 1.0 \text{ mm}$, and 1.2 mm . Scale bars indicate 4 mm .

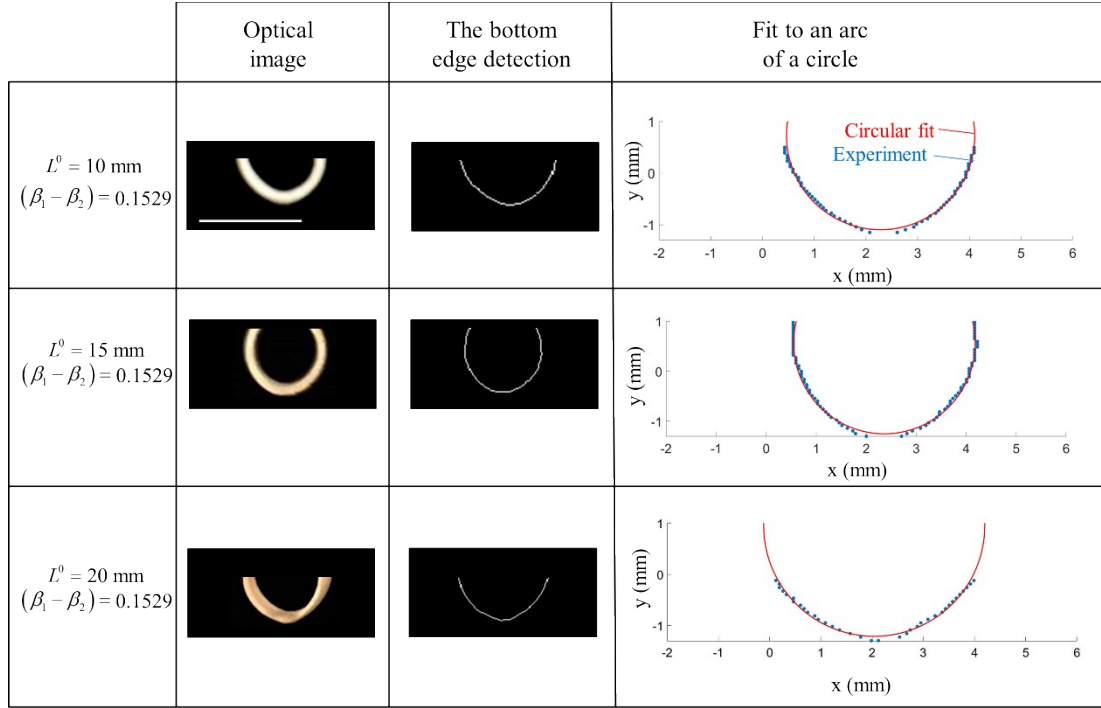


Fig. S9. The optical image, bottom edge detection image, and the MATLAB generated arc fitting image of the bending samples with $w^0 = 2 \text{ mm}$, $t^0 = 0.6 \text{ mm}$, and $(\beta_1 - \beta_2) = 0.1529$ between layers but with $L^0 = 10, 15$, and 20 mm . Scale bars indicate 5 mm .

The folding model:

During folding, the shape changes only occur in a narrow region of the beam with length L_1^0 (**Fig. S10**). After sintering, this length will shrink to L_1^1 (**Fig. S10**), and the folding angle θ can be expressed as:

$$\theta = \frac{L_1^1}{\rho} = \frac{L_1^0 + \Delta L_1^0}{\rho} \quad \text{S10}$$

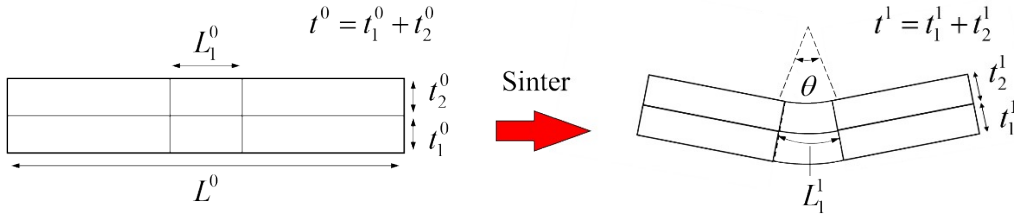


Fig. S10. The notations for the dimensions of the folding samples.

Similar to bending, the length of the line at the connection between the two beams (centerline) must be the same in both beams and therefore:

$$\frac{\Delta L_1^0}{L_1^0} = \beta_1 - \frac{P}{E_1 w^0 t_1^1} - \frac{t_1^1}{2\rho} = \beta_2 + \frac{P}{E_2 w^0 t_2^1} + \frac{t_2^1}{2\rho} \quad \text{S11}$$

By combining Equations S6, S9, and S10, we have:

$$\theta = \frac{L_1^0}{\rho} \left(1 + \beta_1 - \frac{1 + \frac{1}{n} \left(\frac{1}{m} \right)^3 + 3 \left(1 + \frac{1}{m} \right)}{6 \frac{\rho}{t_1^0} \frac{1}{(1 + \beta_1)} \left(1 + \frac{1}{m} \right)} \right) \quad \text{S12}$$

The variable can be rearranged to express Equation S12 as a function of ρ/t^0 for which we have the analytical solution:

$$\theta = \frac{L_1^0}{t^0} \frac{1}{\rho/t^0} \left(1 + \beta_1 - \frac{1 + \frac{1}{n} \left(\frac{1}{m} \right)^3 + 3 \left(1 + \frac{1}{m} \right)}{6 \frac{\rho}{t^0} \frac{1}{(1 + \beta_1)} \left(1 + \frac{1}{m} \right)^2} \right) \quad \text{S13}$$

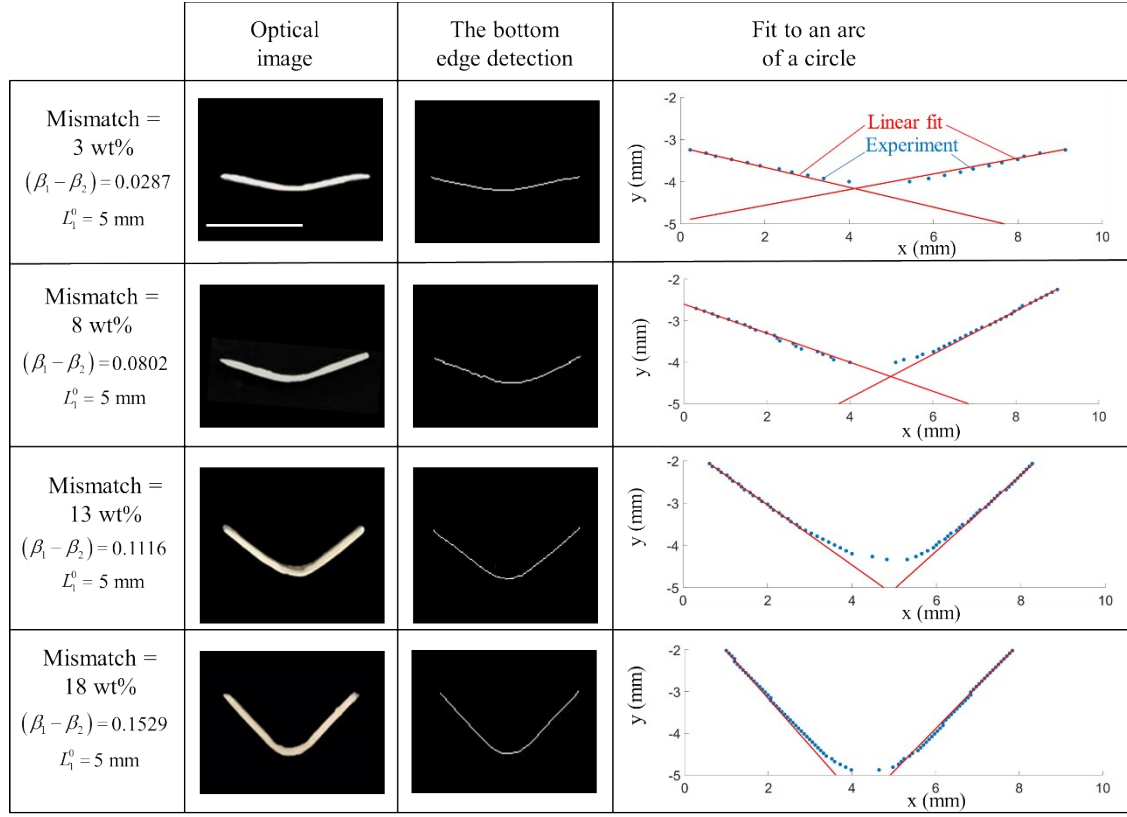


Fig. S11. The optical image, bottom edge detection image, and the MATLAB generated line fitting image of the folding samples with $w^0 = 2$ mm, $t^0 = 0.6$ mm, $L^0 = 15$ mm, $L_1^0 = 5$ mm but with $(\beta_1 - \beta_2) = 0.0287, 0.0802, 0.1116$, and 0.1529 between layers. Scale bars indicate 6 mm.

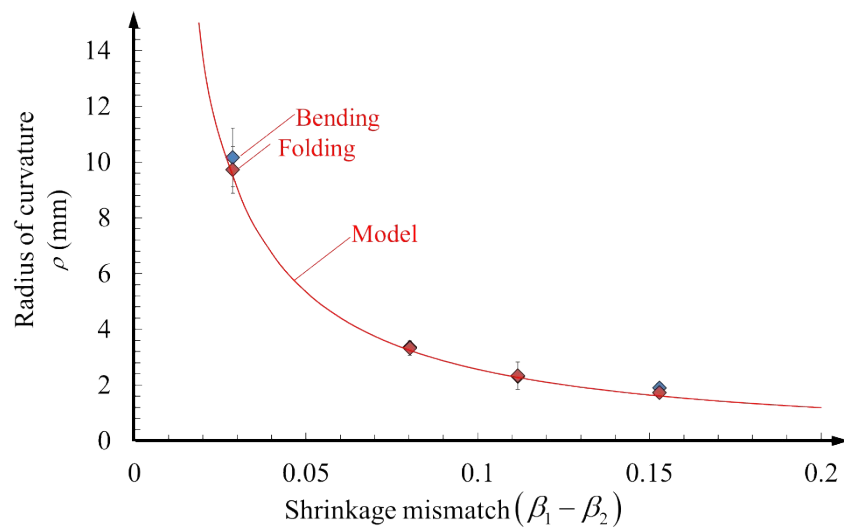


Fig. S12. The correlation between the radius of curvatures measured in mm for both the bending samples and folding samples and the value of shrinkage mismatch $(\beta_1 - \beta_2)$ between layers.

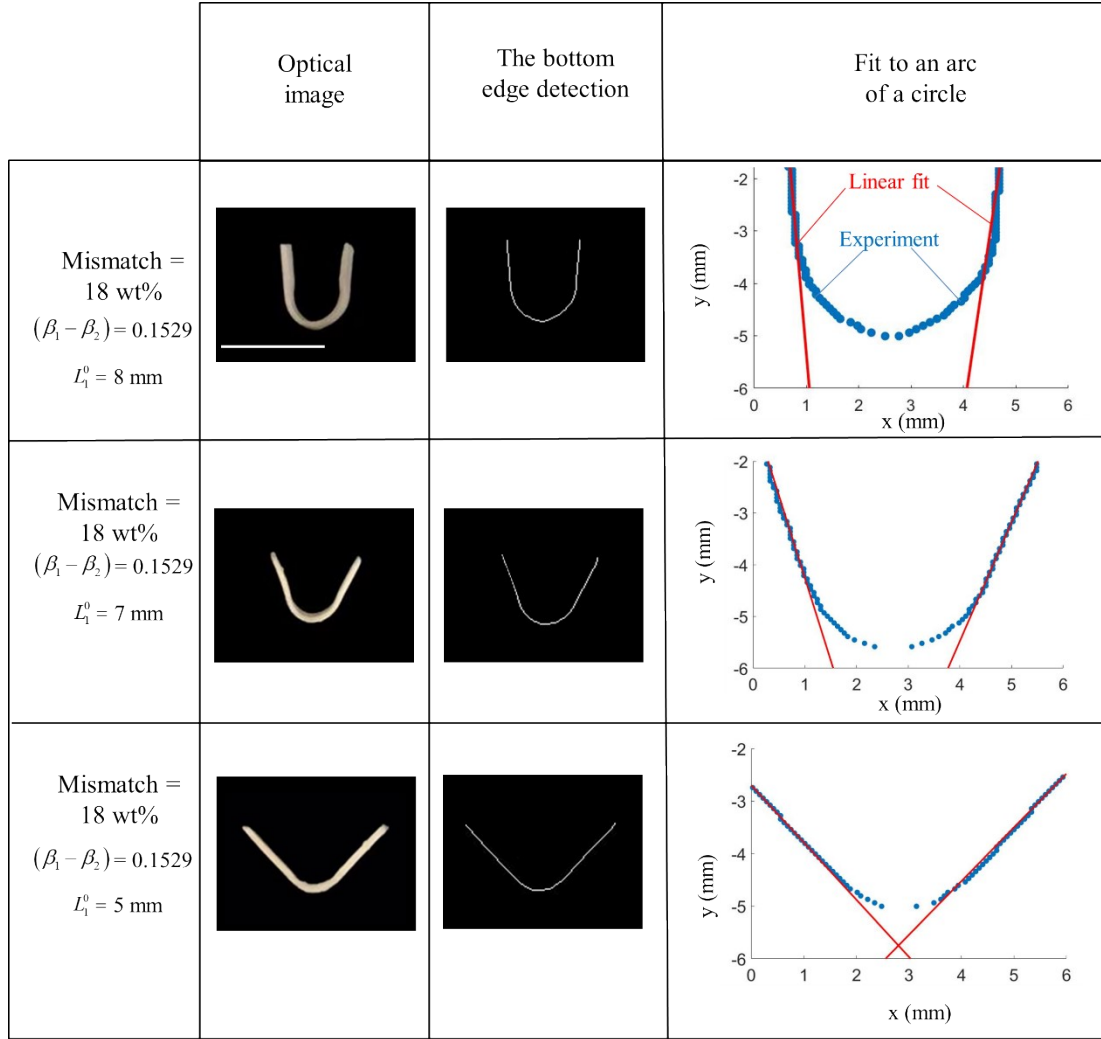


Fig. S13. The optical image, bottom edge detection image, and the MATLAB generated line fitting image of the folding samples with $w^0 = 2$ mm, $t^0 = 0.6$ mm, $L^0 = 15$ mm, $(\beta_1 - \beta_2) = 0.1529$ between layers but with $L_1^0 = 5, 7$, and 8 mm. Scale bars indicate 7 mm.



Fig. S14. The bending sample was made via the replica casting method with resin with 58 wt% alumina particles (Left). The bending sample with $(\beta_1 - \beta_2) = 0.08$ was made via the self-shaped printing method (Right). Scale bar indicates 7 mm.

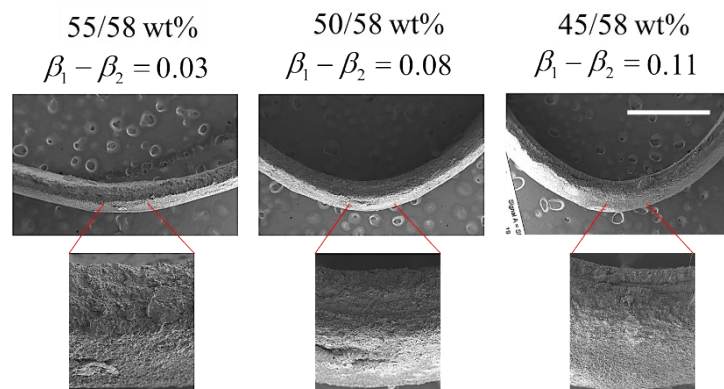


Fig. S15. SEM images of the bending samples with various concentration mismatches, (Top) low magnification (Scale bar 1 mm), (Down) high magnification.

References:

1. S. Timoshenko, *Josa*, 1925, **11**, 233-255.